Article:
Adu-Amankwah, S orcid.org/0000-0002-0568-2093, Black, L orcid.org/0000-0001-8531-4989 and Zajac, M (2022) Application of the Rietveld-PONKCS technique for quantitative analysis of cements and pitfalls of hydration stopping methods. Advances in Civil Engineering Materials, 11 (2). ACEMF9. ISSN 2379-1357

https://doi.org/10.1520/ACEM20210164

Application of the Rietveld-PONKCS technique for quantitative analysis of cements and pitfalls of hydration stopping methods

S. Adu-Amankwah[a], L. Black[a], M. Zajac[b]

[a]Institute for Resilient Infrastructure, School of Civil Engineering, University of Leeds, LS2 9JT, UK

[b]HeidelbergCement Technology Center GmbH, Rohrbacher Str. 95, 69181 Leimen, Germany

ABSTRACT

Existing methods to quantify the degree of hydration of cementitious materials such as selective dissolution and image analysis of scanning electron micrographs are either laborious or unreliable. Meanwhile, quantitative X-ray powder diffraction (QXRD), routinely used to study kinetics and phase evolution of hydrating cements present opportunities to determine quantities of crystalline and poorly-crystalline phases simultaneously. The profile fitting technique however requires structure files, which are non-existent for poorly crystalline materials including most supplementary cementitious materials (SCMs). This contribution is focused upon developing a pseudo-structure file for ground granulated blast furnace slag (GGBS), a Phase of No Known Crystal Structure (PONKCS) for implementation in the Rietveld refinement. Factors affecting the developed model and its stability are assessed. Following, the model is used to quantify the residual GGBS content in hydrated composite cement. The effect of hydration stoppage technique on accuracy of the PONKCS phase is assessed on a binary slag cement. The results show that, the PONKCS phase was stable in synthetic and hydrated cements. Hydration stopping methods that modified the background through decomposition of phase assemblages e.g. freeze-drying also caused overestimation of the PONKCS phase. The QXRD/PONKCS technique is less laborious, has good consistency with the quantified crystalline phase, and enables the degree of hydration of SCMs to be measured alongside hydrated phase assemblages.

1. INTRODUCTION

Quantitative evaluation of the reaction kinetics and products of hydration are fundamental to optimizing the efficiency of cementitious systems and an important step towards widespread utilization of low carbon alternatives to Portland cement. Numerous techniques have been employed to study this e.g. selective dissolution, scanning electron microscopy (SEM), calorimetry, thermogravimetric analysis (TGA), and mass balance calculations [1-6]. These techniques are often coupled to study kinetics of hydration of cementitious materials and to characterize their microstructures.

In most instances, free water in the hydrating cement has to be removed to enable age-dependent studies. Some techniques e.g. mercury intrusion porosimetry (MIP) and SEM require drying of the samples in order to characterize the microstructures of cementitious materials. To this end, different hydration stopping regimes including freeze-drying, vacuum drying and various solvent exchange protocols have been reported and reviewed in the literature [7-9]. These techniques have been shown to influence both the pore structures and hydrated assemblages[10, 11] with the appropriateness of a method dependent on the objective of the microstructural investigation. Regarding phase assemblages, Mitchell and Margeson [12] noted interactions between portlandite and organic solvents, consistent with Beaudoin *et al* [13]. Galan *et al.* [14] reported slight modifications in ettringite contents

after solvent exchange while oven drying was most detrimental. Snoeck *et al.* [15] examined the implications of hydration stopping techniques on bound water and the calcium silicate hydrate (C-S-H) content. The portlandite content was not significantly altered in any of the investigated methods other than freeze-drying and oven drying. Solvent exchange as well as vacuum drying were found to be least detrimental to the C-S-H and the chemically bound water. For the solvent exchange or vacuum drying methods, varied protocols and duration in the solution or vacuum are noticed from the literature [5, 7, 8, 15]. For example, Kakali *et al.* [16] implemented a 24 hour vacuum drying and successfully identified poorly crystalline AFm assemblages in limestone containing cements. Snellings *et al.* [17] removed free water by storing samples in iso-propanol for 7 days followed by storage in a vacuum desiccator. Meanwhile, double solvent exchange involving Iso-propanol (IPA) and diethyl or petroleum ether have been used extensively [18-21] and reported to preserve most phase assemblages. The implications of different hydration stopping methods on the phase contents have not been quantified despite qualitative comparisons in the literature [7, 14].

QXRD is one of the most versatile techniques for simultaneously monitoring reaction kinetics and phase assemblages in cements. However, determination of different amorphous phases in hydrated composite cements including slag and C-S-H by this method is not straightforward. In its current applications, QXRD is not able to distinguish contributions from different amorphous phases and quantification of their relative fractions. Recently, the PONKCS method [22] has been adopted for such purposes [17, 23]. The difficulty associated with the method stems from the fact that amorphous SCMs e.g. fly ash, metakaolin and slag exhibit a halo between 20 and 45 2θ degrees; the same range as the C-S-H, which is the most prevalent phase assemblage in Portland composite cements. Therefore, implementation of a C-S-H model and accounting for the water content in hydrated systems could offer minimize the errors associated with the measurement. However, the accuracy and precision following the application of these are not reported nor the effects of sample preparation. The present study contributes in this respect and discusses other factors that influence accuracy of the quantified poorly crystalline phase.

2. EXPERIMENTAL

Experiments were conducted in two stages – on synthetic mixes of GGBS and corundum in the first instance, and on hydrated cement samples prepared from CEM I, and binary slag cements, designated C and CS respectively. This section first describes the modelling approach and its implementation in the sample sets.

XRD data were acquired on a PANalytical MPD Pro using a CuKα anode operating at 40kV and 40mA, over a range of 5-80 2θ (°). The step size was 0.034 °2θ and nominal time per step of 170.18 seconds, using the scanning X'Celerator detector. A 20 mm diameter sample holder was used on a spinner stage.

Modelling and quantitative XRD analysis was conducted in TOPAS Academic 4.2. The PONKCS phase was modelled from XRD scan on a 100% commercial grade GGBS using the fundamental parameter approach[24]. This defines and fixes the instrument contributions to the diffraction profile. The instrument parameters were 240 mm goniometer radius and active detector length of 2.122 2θ (°) while the incident X-ray beam had a fixed anti-scatter Soller slit with a beam mask of 10 mm and a programmable divergence slit, giving a constant irradiated length of 10 mm and a receiving Soller slit of 2.3°. These parameters were fixed for the modelling and calibration of the poorly crystalline phase and in subsequent refinements.

Modelling of the PONKCS phase was performed on 100 % GGBS XRD scan. A first order Chebyschev polynomial was used to describe the background. Fundamental parameter peak phases were used to model the scattering contribution from GGBS while the small levels of calcite and quartz were refined with the structure files of Maslen[25] and Le Page[26] respectively. The number of peaks was chosen so

that the model accurately described the specimen's diffraction pattern. Following, the peaks were indexed and the best fit space group (in this case Ia-3d cubic) refined as an *hkl* phase using the Pawley method[27]. Deconvolution of the peaks and the resultant GGBS model together with the difference plot and the crystalline phases are illustrated in Figure 1.

The refined lattice parameter a=b=c=15.63 Å, crystallite size and pseudo-density for the modelled GGBS phase were fixed for the calibration step. A synthetic blend of GGBS and corundum (supplied by Sigma Aldrich) prepared at 50:50 GGBS to corundum ratio was used to calibrate the model. This was done by refining the scale factor of the modelled *hkl* phase on the 50:50 XRD scan. Following, a pseudo ZM constant[22] was calculated by re-arranging the internal standard equation (1) and the volume determined from the first stage refinement. Note that the apparent unit cell volume was determined from the lattice parameters. The calculated ZM constant was fixed and stability of the model was evaluated on synthetic mixes of varying GGBS and C-S-H or Corundum.

$$(ZM)_a = \frac{W_a}{W_{st}} \frac{S_{st}}{S_a V_a} (ZMV)_{st} \quad ----(1)$$

Where Z is the number of formula units per unit cell, M and is mass of unit cell, V is unit cell volume, S is scale factor of a phase, W is known weight in %, st denotes the reference standard, and a denotes the GGBS phase under calibration.

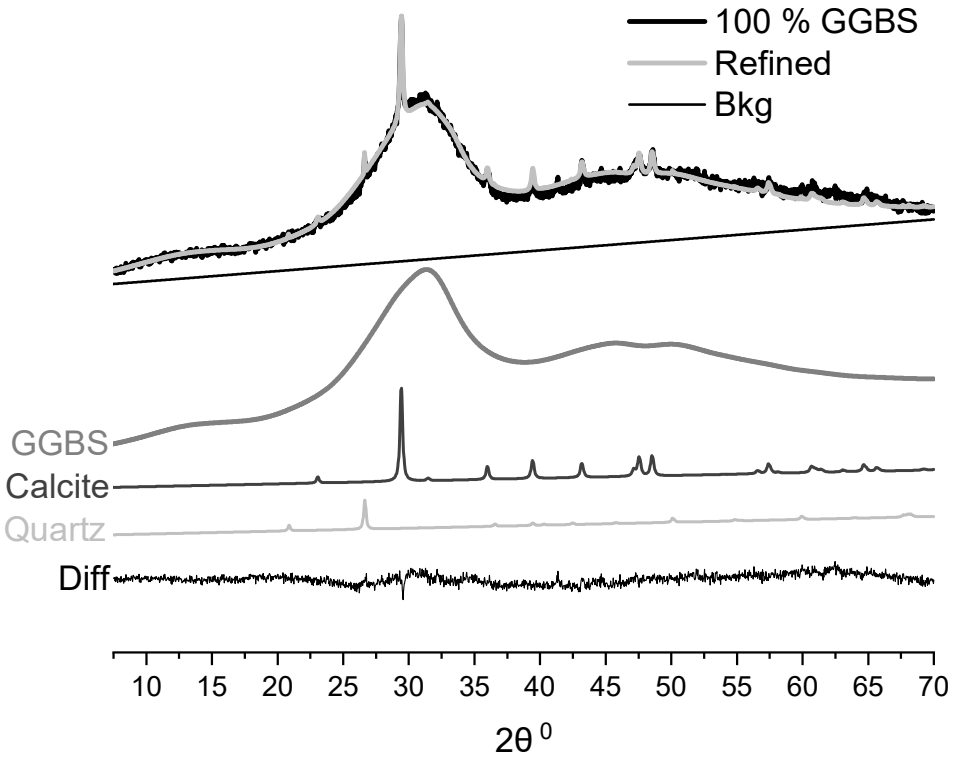

Figure 1 The Modelled GGBS phase for PONKCS calibration and deconvoluted calcite and quartz peaks.

The GGBS PONKCS phase was initially tested on a 50:50 blend of GGBS and 1.5 Ca/Si ratio C-S-H. Details of the C-S-H preparation is detailed elsewhere [28]. Additional synthetic blends of 90:10, 85:15, 40:60, 30:70, and 10:90 GGBS to corundum ratios were prepared to evaluate the model. The objective here was to assess, if the calibrated phase can discriminate between amorphous phases with similar characteristic XRD patterns. Following, two cements: CEM I 52.5 R, and a binary slag cement were investigated. The hydrated systems were prepared at 0.5 w/b ratio and analysed after 1 and 28 days of curing. Four hydration-stopping methods were compared to non-hydration stopped samples.

Details of the hydration stopping techniques are shown in Table 1. The samples were analysed through TGA and XRD.
The protocol for acquiring XRD data on the hydrated samples was the same as that already described for the synthetic samples. The freshly ground non-hydration stopped samples were however covered with Kapton film to prevent drying during the measurement.

Table 1 Details of samples and hydration stopping techniques implemented on the CEM I (C) and the binary slag cement (CS)

Mixes/ hydration stopping regime	C	CS
Freshly ground	√	√
Freeze drying	√	√
IPA (48 hours) + rinsed with ether +20 mins on hot plate at 20 ^{o}C	√	√
IPA (48 hours) + vacuum for 24 hours	√	√
Ground in IPA + rinsed in ether + 20 mins on hot plate	√	√

TGA was performed on the hydrated samples using a Stanton Redcroft 780 Series Analyser under nitrogen gas atmosphere, purged at 58 ml/min. About 16 - 18 mg of freshly ground or hydration stopped sample was heated in a platinum crucible at a rate of 20 °C/minute up to 1000 °C. The bound water content (W_n)was computed between 100 – 550°C in the freshly ground and 20 - 550 °C in the hydration stopped samples according to equations 2. The contents were then normalized to the ignited weight at 550 °C ($M_{550\,^oC}$) to rescale the measured content per 100 g of anhydrous cement.

$$W_n(\%) = \frac{\left(M_{20\,^oC\,(or\,100\,^oC)} - M_{550\,^oC}\right)}{M_{550\,^oC}} * 100\ \%\text{----------} \quad (2)$$

3. RESULTS AND DISCUSSION

Modelling, calibration and testing the PONKCS phase

In hydrated GGBS composite cements, poorly crystalline products of hydration, principally the C-S-H co-exist with unreacted GGBS and both occur around a similar 2θ range. The developed PONKCS phase must therefore be capable of distinguishing between GGBS and other poorly crystalline phases present in the matrix. Figure 2 shows refinement plots of the binary slag and 1.5 Ca/Si ratio C-S-H mixture alongside profiles of other refined phases in the mixture. The crystalline impurities in slag i.e. quartz and calcite were refined using the structure files of Le Page[26] and Maslen[29] respectively, whilst 14 Å tobermorite model (F2dd orthorhombic space group) was used to represent the C-S-H as employed elsewhere[27]. It can be seen that, the modelled GGBS phase clearly differed from the mixed C-S-H. Relative GGBS and C-S-H contents following the refinement were reasonably close to the weighed proportions, thus indicating stability of the model in the synthetic blend. A similar observation was made on a PONKCS phase for metakaolin and C-S-H from matured white Portland cement[17]. Whilst the above suggests the possibility to simultaneously implement models for quantifying multiple poorly crystalline phases such as SCMs and the C-S-H, one must note however, that crystallinity of the C-S-H varies with hydration time[30] and hence could influence accuracy of the PONKCS phase. Notwithstanding, the above described C-S-H model was implemented in the refinement of the hydrated systems investigated in this study.

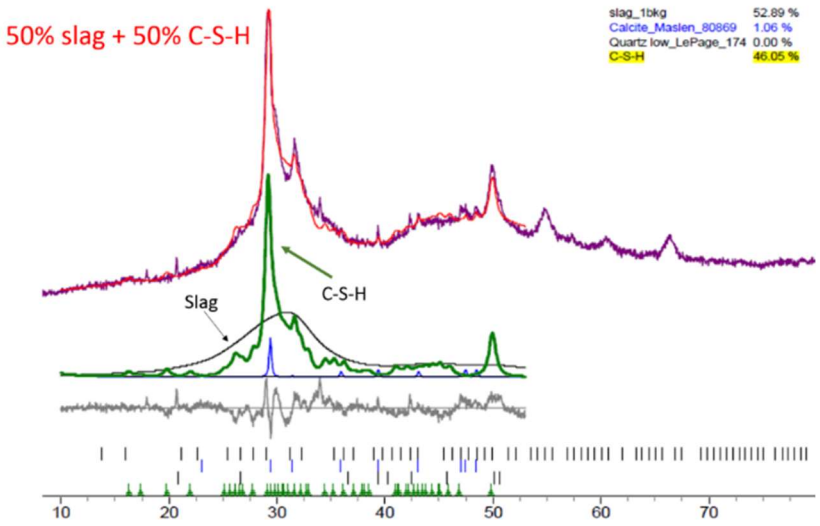

Figure 2 Rietveld refinement of a 1:1 binary GGBS blend with 1.5 Ca/Si C-S-H and deconvolution into the individual contributing phases showing the distinction between GGBS and the C-S-H halos. Output was taken directly from the graphical user interface in TOPAS following the refinement

In addition to being able to distinguish between other poorly crystalline phases in a cement matrix, the modelled PONKCS phase must also be sensitive to changes in the weight fraction of the amorphous phase it seeks to quantify. This was evaluated by formulating anhydrous binary GGBS and corundum mixes at different ratios (i.e. from 10 – 90 % GGBS). Stacked plot of the diffractograms of the investigated specimens are shown in Figure 3. Intensity of the halo varied proportionally as the weight fraction of GGBS in the sample, just as the quartz and calcite impurities. This is explained by the fact that poorly crystalline constituents caused scattering of x-rays and hence, the more of it there was in a sample, the greater the scattering contribution. Another important observation is that, besides intensity, the profile shape of the halo due to GGBS was similar irrespective of its weigh fraction. This means that, a modelled phase capable of adjusting to the x-ray diffraction intensity during profile fitting can constitute a basis for determining the weight fraction of the material present.

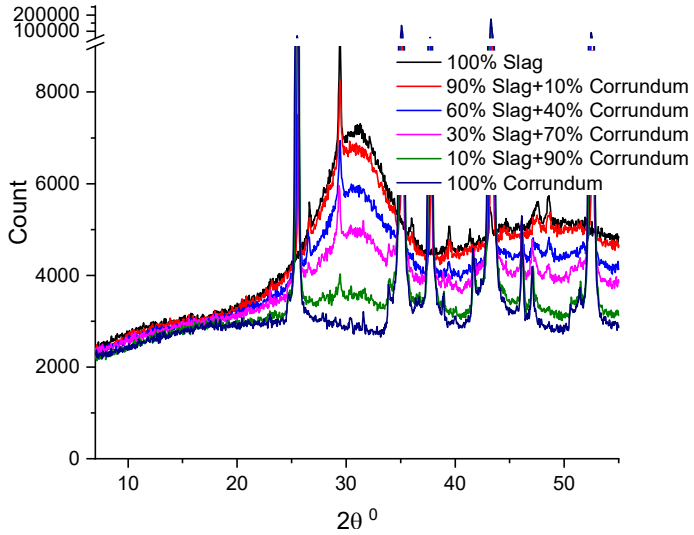

Figure 3 X-ray diffraction patterns of synthetic mixes of GGBS and corundum at different ratios showing consistency of the diffracted halo of GGBS and impurities.

To assess this, the scale factors obtained from the refinement was used together with the pseudo PONKCS phase volume (i.e. automatically computed in the refinement from the lattice parameters)

and the cell mass (i.e. ZM constant from the earlier step) to quantify the weight fraction of the PONKCS phase. Here, we used the external standard method, after[31] and the results shown in Figure 4.

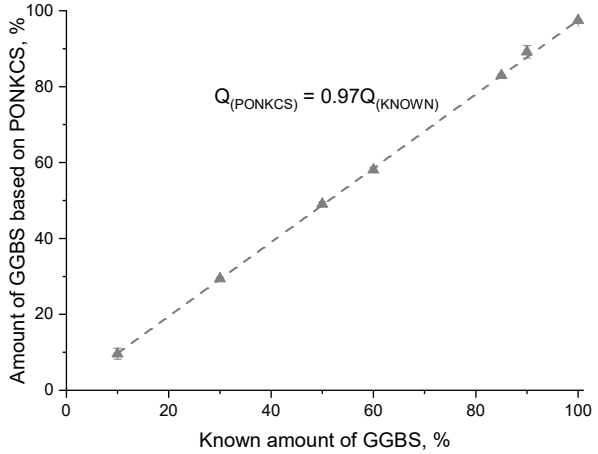

Figure 4 Results of QXRD/PONKCS determination of the weight fraction of GGBS compared to the known quantity in investigated synthetic mixes.

An excellent correlation between the known and quantified amounts of GGBS is obtained, such that the quantified amount was within ±3 % of the known amount of GGBS in the sample. This level of accuracy is typical of QXRD[1] and better than that achievable with the selective dissolution method[6]. Slight discrepancy was seen at high GGBS content due to difficulty in thoroughly dispersing corundum at very high GGBS content. However, such high weight fractions are unlikely to be found in composite cements and should not present significant hindrance in implementing the model.

Effect of water content in the hydrating matrix

Water and multiple poorly crystalline phase assemblages are present in hydrating composite cements, alongside unreacted amorphous SCMs. These can modify the background and consequently affect stability of the modelled phase. Thus, the next step in evaluating the PONKCS phase was to test its quantification accuracy in hydrated composite cements. QXRD analysis of these is best carried out using the external standard method as it overcomes difficulty in homogenizing the hydrated cement paste and the reference standard[31, 32], in this case corundum as well as possible destruction of phase assemblages due to intense homogenization. Formalisation of the external standard determined phase contents however requires consideration of the sample's mass absorption co-efficient (MAC). This can either be measured or calculated based on the linear attenuation coefficient of the individual constituents[33]. Following the method of O'Connor and Raven[31], we estimated this by superposition of the products of linear absorption coefficient of the oxides for the X-ray anode, in this case Cu$k\alpha$ and mass fraction of the oxides as obtained from XRF. X-ray absorption contrast between cement clinker and GGBS is small compared to water and hence the water content present in the matrix can modify the calculated MAC. The different methods for arresting hydration of cementitious materials (see Table 1) however, affect the hydrated phase assemblages and remove to varying extents water in the cements. Therefore, in the results presented in this section, the influence of hydration stopping techniques on stability of the modelled phase was also considered by combining thermal analysis with XRD.

Figure 5 shows DTG for two samples – C and CS, hydrated for 1 or 28 days and subjected to the hydration stopping regimes listed in Table 1. Inserts in the DTG plots are the XRD results focusing on the water-rich phase assemblages present in each sample. Considering these together is essential to understand modifications resulting from the different methods of removing free water from the samples.

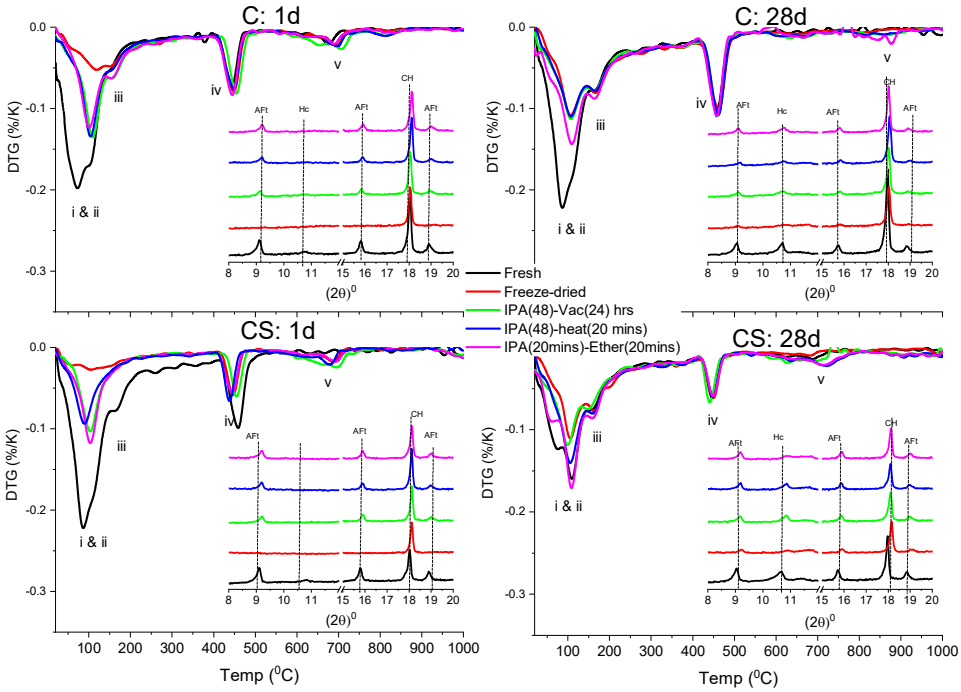

Figure 5 Derivative of the TG curves of CEM I (C) and binary slag cement (CS) showing the effects of hydration stopping method on cement pastes hydrated for 1 or 28 days. Inserts are X-ray diffraction traces showing reflections for ettringite, AFm phases, and portlandite from complementary samples.

The dehydration endotherms numbered i & ii characterized free water, calcium silicate hydrate (C-S-H) and ettringite (AFt). Significant differences were observed amongst the considered hydration stopping methods irrespective of cement type. Greater fraction of free water in the fresh, non-hydration stopped samples after 1 day curing gives the impression of more ettringite. Since these endotherms occur in close proximity to the C-S-H[34], which are also known to be sensitive to vacuum treatment and interaction with organic solvents[7, 8], the XRD peaks provide a clearer basis for interpreting effects of sample treatment on these. The age of the samples influenced sensitivity as noticed from DTG. Water-rich phases seemed more susceptible to being destroyed by the treatment in younger samples. Comparison of the XRD peaks of ettringite indeed show that none of the evaluated water removal techniques preserved these fully. Complete decomposition (based on the crystalline reflections) resulted from freeze-drying and to a greater extent the AFm phases. Meanwhile, effect of solvent exchange seems to be affected also by duration of exposure. Longer storage in IPA and its removal by vacuuming modified intensity of the AFt and AFm peaks. Meanwhile, the portlandite peaks were not affected significantly either in the freshly ground or hydration stopped samples. These observations are in agreement with the RILEM round-robin test[9] and demonstrate that double solvent exchange presented a compromise in preserving most of the phase assemblages whilst minimizing time of exposure to the solvents.

On the 28-day samples, the impact of hydration stopping methods was still notable. Shorter exposure to the organic solvents did not remove all free water even with the double solvent exchange treatment. This could be resolved through further grinding of the sample in IPA to increase the exposed surface area. Differences in the C-S-H & AFt endotherms were small compared to the 1-day samples but freeze-drying was still destructive whilst double solvent exchange was comparable to the non-hydration stopped sample especially in the composite cement. An important consideration during the treatment is potential carbonation of calcium bearing assemblages. Both cements carbonated during the treatment with the 24-hour storage in vacuum desiccator resulting in greater carbonation, which was more critical in younger samples.

Table 2 summarizes the bound water contents and the mass absorption coefficient (in brackets) amongst the cements as a function of hydration time and hydration stopping methods. For both

cements, the bound water content was highest in the freshly ground samples. It is noteworthy that in these samples, bound water was taken as the ignited weight loss between 50 and 550 ^{o}C, normalised to the weight at 550 ^{o}C[35]. Samples from the solvent exchange methods were largely comparable and within ±2 % points of each other. Freeze-drying resulted in consistently lower bound water content. This is consistent with the decomposition of C-S-H, ettringite and carboaluminates as indicated by XRD and DTG. Changes in the X-ray absorption coefficient are discussed in the section that follows.

Table 2 The bound water and MAC (within brackets) as a function of hydration stopping method after 1 and 28d

Mix	Age	Hydration stopping methods				
		Fresh	Freeze-dried	IPA(48)+ Vac (24) hrs	IPA(48hrs)+Ether +heat(20 mins)	IPA(20min)+Ether +heat (20 mins.)
C	1	20.3(66.5)	12.3(85.6)	17.5(82.2)	15.9(83.2)	17.1(82.5)
	28	28.0(66.5)	24.8(77.9)	24.0(78.4)	24.1(78.4)	26.9(76.9)
CS	1	15.5(59.6)	6.4(79.9)	10.8(77.2)	10.6(77.3)	11.3(76.9)
	28	24.0(59.6)	18.7(72.7)	22.3(70.9)	21.2(71.4)	22.9(70.6)

Figure 6 shows x-ray diffraction patterns of the binary slag blend cured for 1 and 28 days and hydration stopped by the above methods. The same data collection regime was used for all samples and plausible effects of tube ageing would be captured in the scale factor of the reference material and hence the G-factor for calculating the phase contents. The background was highest in the freshly ground samples while the hydration stopped samples were similar for the considered ages. The high background is not attributable to the x-ray tube anode nor ageing since the scans overlapped at low angles up to 9 2θ (°). It is also noteworthy that instrument parameters e.g. generator settings, sample holder, beam masking etc. could modify the background, but these were fixed for our data collection regime. Additionally, sample grinding could equally modify the background due to amorphization. In the data presented here, similarly aged samples were ground to pass 45µ sieve before XRD scans and hence potential amorphization would be consistent amongst the samples. Consequently, the distinctively higher background in the freshly ground samples may be attributed to X-ray scattering by free water. Slightly higher background in the range where the hump corresponding to slag occurred i.e. 20 – 60 °(2θ) was observed in the freeze-dried sample, but at low angle, the background was much lower in the sample subjected to 48 hours in IPA plus 24 hours vacuuming. Such differences are explained on the basis of the bound water content, but the results were repeatable.

In the quantitative XRD analysis, water in the specimen is considered through the mass attenuation or absorption co-efficient (MAC). This depends on the types of atoms present (i.e. total atomic cross section) and atomic mass unit (i.e. relative abundance of elements)[36] in the sample, which in turn determines intensity of the reflected x-rays[37]. These constants are available from crystallographic tables and by knowing the proportion of constituent oxides, the MAC of the mixture is computed by superposition according to equation 2.

Among the oxides in cements, H_2O and CO_2 have the lowest linear absorption coefficient. However, the amount of water, free and bound in cement pastes are usually high and as a result influence the MAC significantly as shown in Table 2. Note that, the MAC is directly proportional to the weight fraction of the phase and hence, a quantified phase could have more than 10 % error without correcting for the sample MAC. Water content in the matrix was accounted for in the quantification and subsequently used to scale the weight fractions to 100 g of paste as recommended in Snellings[38]. In the freshly ground non-hydration stopped samples, the water content was taken as the mixing water (i.e. 33 % of water in the matrix) whilst that in the hydration stopped samples were taken as the bound water as shown in Table 2 and combined with those from cement, slag and their relative concentrations.

$$\mu_{sample} = \sum \frac{w_p \mu_p}{W} - - - - (2)$$

Where μ_{sample} is MAC of sample, μ_p is MAC of a given oxide, p; w is weight fraction of an oxide as determined by XRF and TGA (for bound water); and W is total weight of all oxides in the matrix.

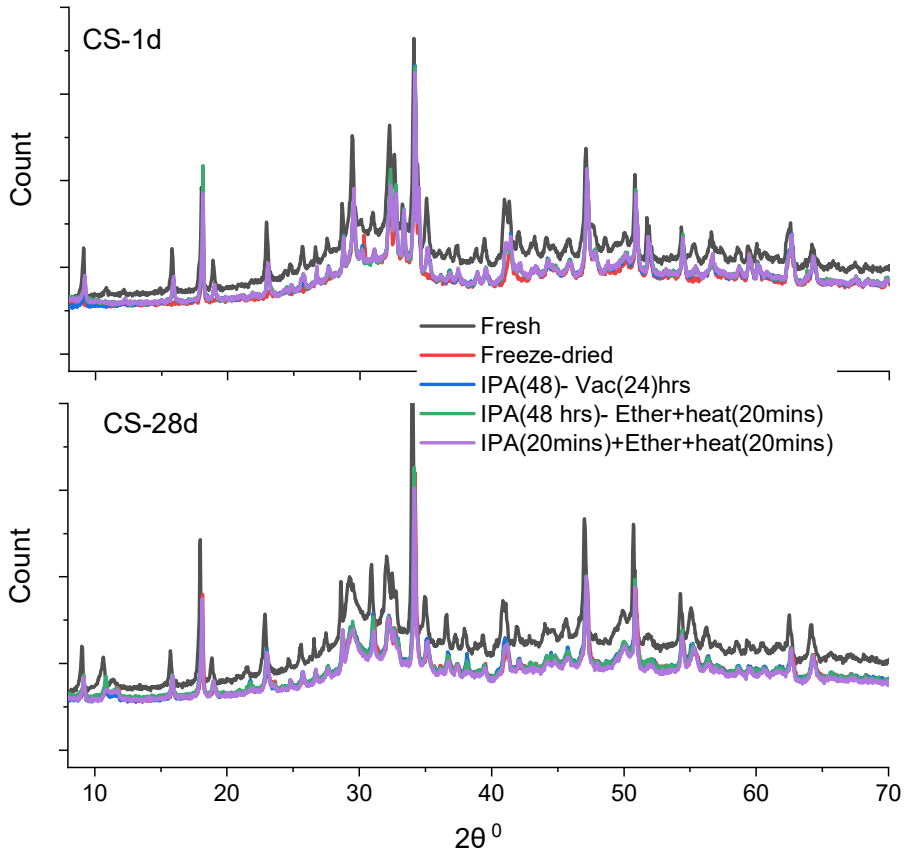

Figure 6 XRD diffraction patterns of binary slag blend subjected to different hydration stopping methods cured for 1 and 28 days.

Following determination of the MAC for each specimen (μ_{sample}), the weight fractions of residual and hydrated phases (W_a) were calculated using the scale factors (S_a) of individual phases obtained directly from the Rietveld refinement. Equation 3 links the scale factor, sample's MAC, crystallographic parameters (ρ and v) of the phase of interest including the PONKCS phase and that of a reference standard (i.e. in this case corundum) according to the external standard method[31, 32]. The starting structures for the crystalline clinker phases were based on the ICSD database.

$$W_a = S_a \frac{\rho_a v_a^2 \mu_{\text{sample}}}{G} - - - - (3)$$

The calibration factor, G is obtained from equation 4 using the unit cell density, ρ_{st} and volume v_{st} together with the MAC for the external standard, corundum, μ_{st}; its known weight of (purity) W_{st} and the refined scale factor of the 100% corundum sample, S_{st} scanned using the same data acquisition protocol as already described in the experimental section. In this work, the reference standard was scanned once on each data collection date, before scanning the cement samples using the same acquisition parameters. Purity of the corundum used in the investigation was 98 %.

$$G = S_{st} \frac{\rho_c v_{st}^2 \mu_{st}}{W_{st}} - - - - (4)$$

Figure 7 shows the effect of hydration stopping method on the degree of hydration of the clinker component in the neat and binary cements after 1 and 28 days. Despite differences in the refined scale factors of the clinker minerals, the degree of clinker hydration calculated as the difference between unreacted clinker phases (i.e. sum of C_3S, C_2S, C_3A and C_4AF) in the sample and the initial amount in the anhydrous sample expressed as percentage of the former[1, 3] were comparable in the individual mixes.

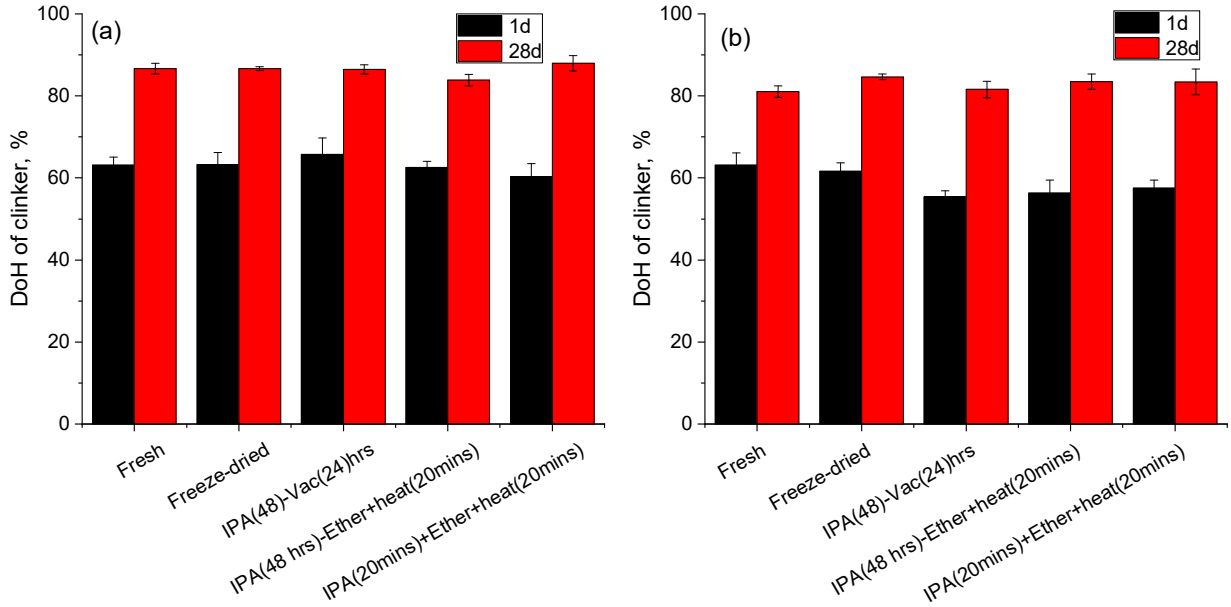

Figure 7 Degree of hydration of the clinker phases in (a) neat cement and (b) binary slag cement showing the effect of hydration stopping method on the quantification and error bars of the quantification. Note: The error ranges in the phase contents of the individual clinker phases for duplicate runs were 1 - 2 % in both sets of samples.

The standard deviation associated with two independent measurements on similarly conditioned samples from the same bulk cement pastes and indicated as error bars in the plots were random amongst the different hydration stopping techniques, suggesting internal consistency of the results. However, magnitude of the error bar seemed much smaller in the freeze-dried samples in both datasets. Errors arising from quantification of the degree of hydration due to sample preparation was suggested as possible pitfall of QXRD in Scrivener *et al.*[3]. Notwithstanding, the data shows that the impact of hydration stopping on quantification of the clinker phases was not significant. It is noteworthy that the dilution effect of slag at 50 % clinker replacement did not necessarily lead to greater degree of clinker hydration even at early age. This is plausibly due to faster reaction of slag used in the investigation[20] and the fact that slag does not provide active nucleation substrate for C-S-H growth[39].

Refinement plots of the 28-day samples showing the observed XRD patterns, calculated model structures (designated refined), background (designated bkg) and deconvoluted contributions from the GGBS PONKCS phase, C-S-H, refined crystalline phases and resultant difference plots are shown in Figure 8a and 8b for the freshly ground and freeze-dried samples respectively. The Kapton film contribution to the background of the freshly ground sample is also shown in Figure 8a. The refined weighted pattern (Rwp) for the two datasets were < 5 and together with the narrow difference plots show a very good fit of the observed data.

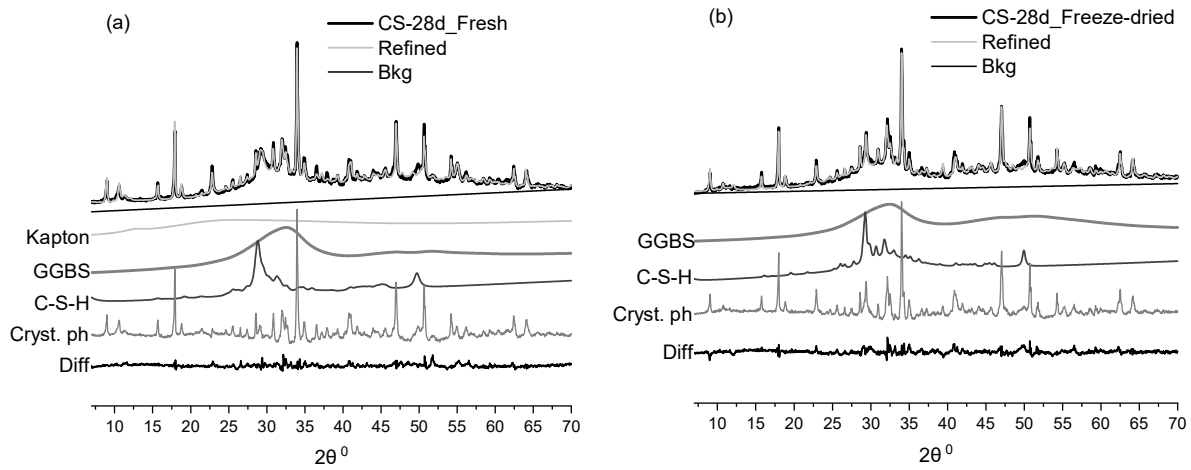

Figure 8 XRD patterns of mix CS hydrated for 28-days (a) freshly ground without hydration stopping and (b) hydration stopped by freeze-drying. The observed and calculated (refined) patterns are superimposed whilst contributing structures/patterns from the GGBS PONKCS phase, C-S-H and crystalline phases are deconvoluted.

Results of the implemented PONKCS phase for quantifying the residual GGBS content and hence the degree of its hydration in the binary slag cement is shown in Figure 9 for 1 and 28 day cured cement paste samples. It should be noted that these systems were more complex due to prevalence of multiple poorly crystalline phase assemblages e.g. C-S-H and AFm. We showed in the earlier section that the developed PONKCS phase was capable of distinguishing between the C-S-H and GGBS. Consequently, the scale factors for slag after the refinement (shown in Figure 8) were used with the corresponding sample's MAC and G-factors of the reference to determine the residual slag contents. The sample MAC as shown in Table 2 were used in calculating the phase content. As illustrated in Figure 9, for the same aged samples, the scale factors of the slag phase after the refinement, indicative of the relative weight fraction of the phase in the sample differed with the hydration stopping techniques. Plausibly, effects or rather artefacts from the treatment as well as performance loss of the x-ray tube due to ageing could be the reasons for the difference in scale factors at 1 and 28 days. X-ray tube ageing is corrected in the quantification by using the same data acquisition protocol for the reference sample and the specimens such that X-ray errors are assumed to be consistent among these and should cancel out as shown in equation 3[31, 32].

The degree of hydration calculated similarly as for the clinker phases by expressing the reacted slag content as percentage of the initial amount showed clear sensitivity to hydration stopping methods. Differences among the solvent exchanged samples were statistically insignificant and fell within the error margins except the freeze-dried samples, which showed consistently lower degree of hydration. The difference was much larger in the younger samples, which may be explained by the decomposition of water-rich assemblages as noted from DTG and XRD in Figure 5. This is consistent with previous studies on methods for arresting hydration in cements[7, 8, 14, 15], which also reported phase decomposition upon freeze-drying or vacuum treatment. The decomposed phases interfere with the background of the diffractogram, which reduce accuracy of analysing poorly crystalline phases quantitatively.

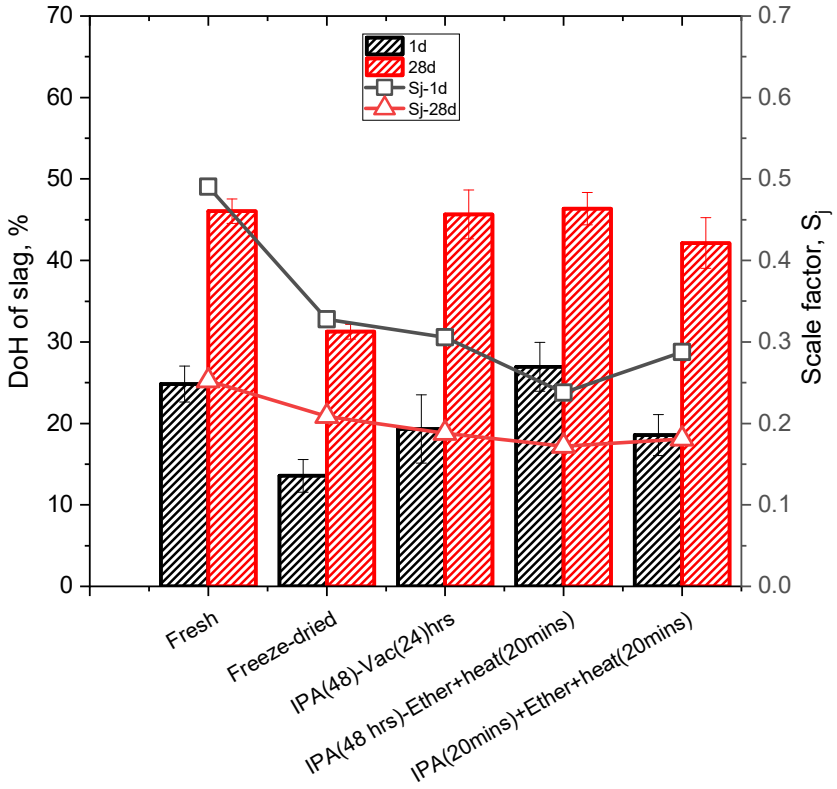

Figure 9 Scale factor after Rietveld refinement (line and symbols) and calculated degree of hydration of slag (columns) for binary cement paste samples cured for 1 or 28 days and hydration stopped by the investigated techniques.

4. CONCLUDING REMARKS

We have reported in this paper modelling of the X-ray diffraction pattern of GGBS, a poorly crystalline supplementary cementitious material. The model was calibrated and tested on synthetic mixes of GGBS with varying proportions of corundum as well as GGBS and 1.5 calcium to silicon ratio C-S-H. We have shown that the modelled phase can quantify the GGBS content even when other poorly crystalline phases were present in the mixture.

On hydrated samples using the external standard method, we were able to implement the PONKCS phase alongside structure files of identified crystalline phases, predominantly unreacted clinker phases and hydrated assemblages. We showed that, once X-ray attenuation was accounted for, the hydration stopping techniques did not affect the clinker phases significantly. This implies that degree of cement clinker hydration could be determined accurately following any of the investigated hydration stopping techniques or even on freshly ground hydrated cement samples.

The modelled PONKCS phase was successfully used to quantify the residual GGBS content after 1 and 28 days of curing and eventually the degree of hydration. The error margins associated with the measurement would be expected to be greater in hydrated composite cements compared to the synthetic mixes due to multiple amorphous phases. In the present study, quantification of independently measured samples lead to ± 3% error in the quantified degree of hydration. This is typical of quantitative powder X-ray diffraction even for crystalline phases.

Based on the results presented here, the PONKCS technique can be applied on freshly ground non-hydration stopped samples as well as hydrations stopped ones. Drying during the data acquisition must be avoided e.g. by using Kapton film. On the hydration stopped samples, accurate determination of the bound water is required when performing QXRD on hydration stopped samples. Excessive

drying of the sample affected accuracy of quantification of the PONKCS phase and particularly, freeze-drying was found to be unsuitable.

Despite the advantages of enabling kinetics of hydration and phase assemblage evolution to be followed simultaneously, the PONKCS method has some drawbacks. It is sensitive to factors that modify the background of the X-ray diffractogram or overlapping amorphous phases. It also requires specimens to have been scanned using the same data collection protocol and instrument. More work is needed to generate a sample structure file that may be independent of the instrument for extended application. Moreover, there is the need for independent validation of the refinement results. For the data reported here, SEM data published elsewhere[20] provides validation for the quantified degree of hydration. Such verifications are necessary to instil confidence in the results. We recommend inter-laboratory calibration of extensive datasets as means of improving confidence in the PONKCS technique.

REFERENCES

[1] V. Kocaba, E. Gallucci, K.L. Scrivener, Methods for determination of degree of reaction of slag in blended cement pastes, Cement and Concrete Research, 42 (2012) 511-525.

[2] K.L. Scrivener, Backscattered electron imaging of cementitious microstructures: understanding and quantification, Cement and Concrete Composites, 26 (2004) 935-945.

[3] K.L. Scrivener, T. Füllmann, E. Gallucci, G. Walenta, E. Bermejo, Quantitative study of Portland cement hydration by X-ray diffraction/Rietveld analysis and independent methods, Cement and Concrete Research, 34 (2004) 1541-1547.

[4] K. Scrivener, B. Lothenbach, N. De Belie, E. Gruyaert, J. Skibsted, R. Snellings, A. Vollpracht, TC 238-SCM: Hydration and microstructure of concrete with SCMs, Materials and Structures, 48 (2015) 835-862.

[5] P.T. Durdziński, M. Ben Haha, S.A. Bernal, N. De Belie, E. Gruyaert, B. Lothenbach, E. Menéndez Méndez, J.L. Provis, A. Schöler, C. Stabler, Z. Tan, Y. Villagrán Zaccardi, A. Vollpracht, F. Winnefeld, M. Zając, K.L. Scrivener, Outcomes of the RILEM round robin on degree of reaction of slag and fly ash in blended cements, Materials and Structures, 50 (2017) 135.

[6] K. Luke, F.P. Glasser, Selective dissolution of hydrated blast furnace slag cements, Cement and Concrete Research, 17 (1987) 273-282.

[7] N.C. Collier, J.H. Sharp, N.B. Milestone, J. Hill, I.H. Godfrey, The influence of water removal techniques on the composition and microstructure of hardened cement pastes, Cement and Concrete Research, 38 (2008) 737-744.

[8] J. Zhang, G.W. Scherer, Comparison of methods for arresting hydration of cement, Cement and Concrete Research, 41 (2011) 1024-1036.

[9] R. Snellings, J. Chwast, Ö. Cizer, N. De Belie, Y. Dhandapani, P. Durdzinski, J. Elsen, J. Haufe, D. Hooton, C. Patapy, M. Santhanam, K. Scrivener, D. Snoeck, L. Steger, S. Tongbo, A. Vollpracht, F. Winnefeld, B. Lothenbach, Report of TC 238-SCM: hydration stoppage methods for phase assemblage studies of blended cements—results of a round robin test, Materials and Structures, 51 (2018) 111.

[10] R.F. Feldman, J.J. Beaudoin, Pretreatment of hardened hydrated cement pastes for mercury intrusion measurements, Cement and Concrete Research, 21 (1991) 297-308.

[11] C. Gallé, Effect of drying on cement-based materials pore structure as identified by mercury intrusion porosimetry: A comparative study between oven-, vacuum-, and freeze-drying, Cement and Concrete Research, 31 (2001) 1467-1477.

[12] L.D. Mitchell, J.C. Margeson, Theeffects of solvents on C–S–H as determined by thermal analysis, Journal of Thermal Analysis and Calorimetry, 86 (2006) 591-594.

[13] J.J. Beaudoin, P. Gu, J. Marchand, B. Tamtsia, R.E. Myers, Z. Liu, Solvent Replacement Studies of Hydrated Portland Cement Systems: The Role of Calcium Hydroxide, Advanced Cement Based Materials, 8 (1998) 56-65.

[14] I. Galan, H. Beltagui, M. García-Maté, F.P. Glasser, M.S. Imbabi, Impact of drying on pore structures in ettringite-rich cements, Cement and Concrete Research, 84 (2016) 85-94.
[15] D. Snoeck, L.F. Velasco, A. Mignon, S. Van Vlierberghe, P. Dubruel, P. Lodewyckx, N. De Belie, The influence of different drying techniques on the water sorption properties of cement-based materials, Cement and Concrete Research, 64 (2014) 54-62.
[16] G. Kakali, S. Tsivilis, E. Aggeli, M. Bati, Hydration products of C3A, C3S and Portland cement in the presence of CaCO3, Cement and Concrete Research, 30 (2000) 1073-1077.
[17] R. Snellings, A. Salze, K.L. Scrivener, Use of X-ray diffraction to quantify amorphous supplementary cementitious materials in anhydrous and hydrated blended cements, Cement and Concrete Research, 64 (2014) 89-98.
[18] A. Machner, M. Zajac, M. Ben Haha, K.O. Kjellsen, M.R. Geiker, K. De Weerdt, Chloride-binding capacity of hydrotalcite in cement pastes containing dolomite and metakaolin, Cement and Concrete Research, 107 (2018) 163-181.
[19] A. Schöler, B. Lothenbach, F. Winnefeld, M. Zajac, Hydration of quaternary Portland cement blends containing blast-furnace slag, siliceous fly ash and limestone powder, Cement and Concrete Composites, 55 (2015) 374-382.
[20] S. Adu-Amankwah, M. Zajac, C. Stabler, B. Lothenbach, L. Black, Influence of limestone on the hydration of ternary slag cements, Cement and Concrete Research, 100 (2017) 96-109.
[21] F. Deschner, F. Winnefeld, B. Lothenbach, S. Seufert, P. Schwesig, S. Dittrich, F. Goetz-Neunhoeffer, J. Neubauer, Hydration of Portland cement with high replacement by siliceous fly ash, Cement and Concrete Research, 42 (2012) 1389-1400.
[22] N.V.Y. Scarlett, I.C. Madsen, Quantification of phases with partial or no known crystal structures, Powder Diffraction, 21 (2006) 278-284.
[23] G.V.P.B. Singh, K.V.L. Subramaniam, Quantitative XRD Analysis of Binary Blends of Siliceous Fly Ash and Hydrated Cement, Journal of Materials in Civil Engineering, 28 (2016) 04016042.
[24] R.W. Cheary, A.A. Coelho, J.P. Cline, Fundamental Parameters Line Profile Fitting in Laboratory Diffractometers, J. Res. Natl. Inst. Stand. Technol., 109 (2004) 1-25.
[25] E. N. Maslen, V. A. Streltsov, N.R. Streltsova, X-ray study of the electron density in calcite, CaCO3, Acta Cryst., B49 (1993) 636-641.
[26] Y.L. Page, G. Donnay, Refinement of the crystal structure of low-quartz, Acta Cryst., B32 (1976) 2456-2459.
[27] G.S. Pawley, Unit-cell refinement from powder diffraction scans, J. Appl. Cryst., 14 (1981) 357-361.
[28] E. Tajuelo Rodriguez, K. Garbev, D. Merz, L. Black, I.G. Richardson, Thermal stability of C-S-H phases and applicability of Richardson and Groves' and Richardson C-(A)-S-H(I) models to synthetic C-S-H, Cement and Concrete Research, 93 (2017) 45-56.
[29] E.N. Maslen, V.A. Streltsov, N.R. Streltsova, X-ray study of the electron density in calcite, CaCo3, Acta Crystallographica Section B, 49 (1993) 636-641.
[30] S.T. Bergold, F. Goetz-Neunhoeffer, J. Neubauer, Quantitative analysis of C–S–H in hydrating alite pastes by in-situ XRD, Cement and Concrete Research, 53 (2013) 119-126.
[31] B.H. O'Connor, M.D. Raven, Application of the Rietveld Refinement Procedure in Assaying Powdered Mixtures, Powder Diffraction, 3 (1988) 2-6.
[32] D. Jansen, F. Goetz-Neunhoeffer, C. Stabler, J. Neubauer, A remastered external standard method applied to the quantification of early OPC hydration, Cement and Concrete Research, 41 (2011) 602-608.
[33] D.C. Creagh, J.H. Hubbell, X-ray absorption (or attenuation) coefficients, International Tables for Crystallography, C (2006) 220-229.
[34] V.S. Ramachandran, R.M. Paroli, J.J. Beaudoin, A.H. Delgado, Handbook of Thermal Analysis of Construction Materials, NOYES Publications, 2002, pp. 455 - 459.

[35] B. Lothenbach, P. Durdziński, K.D. Weerdt, Thermogravimetric analysis, in: R.S. Karen Scrivener, Barbara Lothenbach (Ed.) A Practical Guide to Microstructural Analysis of Cementitious Materials, CRC Press, Boca Raton, 2016, pp. 117 - 208.
[36] J.H. Hubbell, Review and history of photon cross section calculationsWork supported by the National Institute of Standards and Technology, Physics in medicine and biology, 51 (2006) R245.
[37] L. Alexander, H.P. Klug, Basic Aspects of X-Ray Absorption in Quantitative Diffraction Analysis of Powder Mixtures, Analytical Chemistry, 20 (1948) 886-889.
[38] R. Snellings, X-ray powder diffraction applied to cement, in: R.S. Karen Scrivener, Barbara Lothenbach (Ed.) A Practical Guide to Microstructural Analysis of Cementitious Materials, CRC Press, Boca Raton, 2016, pp. 108 - 162.
[39] E. Berodier, K. Scrivener, Understanding the filler effect on the nucleation and growth of C-S-H, Journal of the American Ceramic Society, 97 (2014) 3764-3773.